Journal of Fluorescence
https://doi.org/10.1007/s10895-023-03146-x

RESEARCH

Effect of cyclodextrins inclusion complexes into absorption and emission spectra of P-methylaminobenzoate derivatives: A DFT and TD-DFT investigation

Sonia Badi[1,2] · Fatiha Madi[1] · Leila Nouar[1] · abdelhak Gheid[2]

Received: 24 November 2022 / Accepted: 9 January 2023

Abstract
In this study, density functional theory (DFT) and time-dependent DFT (TD-DFT) studies of methyl 4-aminobenzoate and methyl 4- amino-2-hydroxybenzoate and their inclusions complexes with α and γ-cyclodextrins were applied to control the effect of cyclodextrins on the absorption and emission properties of P-methylaminobenzoate derivatives. Absorption and emission spectra of free and encapsulated P-methylaminobenzoate derivatives were successfully analysed and compared with experimental results. Interestingly, conformational changes between ground and excited states of both fluorophores were also studied.

Keywords B3LYP-D3/ cc-pVDZ · TD-DFT/B3LYP/6-31G(d) · P-methylaminobenzoate derivatives · α and γ-CDs · Absorption and emission

Introduction

Recently, several studies have been focused on investigating the different fluorescent properties of dyes in inclusion complexes with cyclodextrins and cucurbit[n]uril. The change in the different fluorescent characteristics of the studied dyes after Host–Guest interaction is significant [1–5].

Sueishi et al. [6] has studied fluorescence quantum yields of 4-substituted N-methylphthalimides by inclusion complexation with native β-CD and 2,6-methylated β-CDs. Moreover, they found that the quantum yields values of the N-methyl-phthalimides having D–A characteristics were significantly improved by the inclusion of β-CDs, and the local polarity around the D–A N-methylphthalimides plays a significant role in the improvement of the quantum yields values of the CD inclusion complexes.

Sueishi et al. [7] also studied the inclusion complexation of a fluorescent probe [4′,6-diamidino-2-phenylindole (DAPI)] using various cyclodextrins (CDs) and cucurbit[7] uril (CB7). They found that quantum yields values of DAPI were significantly greater upon its inclusion by CB7 and augmented as the empirical solvent polarity parameter (ET(30)) diminished. Centred on these results, they concluded that the polarity of the microenvironment and protonation ability of the excited state of DAPI play essential roles in emission efficiency.

Fluorescence behaviour of Tramadol hydrochloride inside β-CD at high concentration was investigated by Zidane et al. [8]. They characterize the occurrence of inhibition of self-quenching by inclusion of fluorescence emitters inside the hydrophobic cavity of β-cyclodextrin (β-CD); Complexation

Highlights
- DFT and TD-DFT methods were successfully applied to obtain ground andexcited states geometries of P-methylaminobenzoate derivatives guests and theirinclusion complexes (1:1) with α and γ-CDs.
- Largely modification of absorption and emission spectra of methyl4-aminobenzoate (guest 1) and methyl 4- amino-2-hydroxybenzoate (guest2) were observed after interactionswith CDs.
- The presence of two overlapping bands onabsorption and emission spectra confirm the formation of inclusion complex.

✉ Fatiha Madi
madi.fatiha@univ-guelma.dz

[1] Laboratory of Computational Chemistry and Nanostructures, Department of Material Sciences, Faculty of Mathematical, Informatics and Material Sciences, University of 8 Mai 1945, Guelma, Algeria

[2] Laboratory of Water and Environmental Sciences, Department of Material Sciences, Faculty of Technology and Sciences, Messadia Med Cherif University, Souk Ahras, Algeria

Published online: 09 February 2023

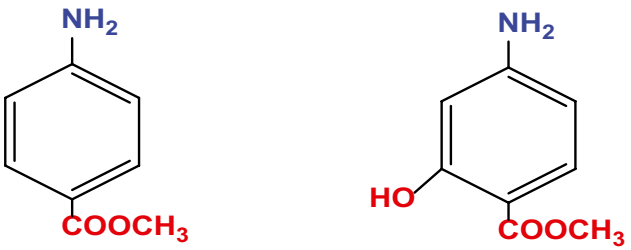

Guest 1 *Guest 2*

Fig. 1 Chemical structures of methyl 4-aminobenzoate (G1) and methyl 4- amino-2-hydroxybenzoate (G2)

of Tramadol by β-CD does not cause modification of its absorbance and fluorescence spectra.

The steady state and time-resolved fluorescence study of 2-amino-4,6-dimethyl pyrimidine (ADMP) have been studied in aqueous solution of α- and γ-cyclodextrins (CDs) [9]. The experimental data point out the formation of 1:1 complexes of ADMP with α- and γ-CDs. The inclusion process determines an enhancement of the fluorescence, but an insignificant shift in the position of the fluorescence band. The results indicate that both the hydrophobic cavity and the hydrogen bonding between ADMP and water are the dominant factors in the controlling the photochemistry of ADMP in α- and γ-CD complexes.

methyl 4-aminobenzoate and methyl 4- amino-2-hydroxybenzoate (Fig. 1) are fluorophores recognized by their spectral emission dependent on their environment, their photophysical and photochemical properties are largely influenced in the presence of solvent or formation of inclusion complexes. Marek [10] and Karolina and Marek [11] explores Steady-State and time resolved spectroscopic techniques to study P-methylaminobenzoate derivatives and their inclusions complexes with α and γ-cyclodextrins in mixtures of solvent THF-H2O. They observed non linear solvatochromic shifts of the absorption and fluorescence bands for both fluorophores. This non linearity has been explained in terms of the non-specific dielectric enrichment of the solvent around the polar solute.

In the present study, we explore by DFT and TD-DFT powerful calculations, electronics and UV–visible spectroscopic properties of free methyl 4-aminobenzoate and methyl 4- amino-2-hydroxybenzoate and their inclusion complex with α and γ-CDs. The aim of this computational investigation is to give more information about conformation and molecular orbitals modification due to intermolecular interactions of different studied species in both ground and excited states leading to absorption and emission properties change and to make comparison with experimental results.

Computational details

Both P-methylaminobenzoate derivatives and their inclusions complexes (1:1) were constructed according to the methodology described previously [12]. Two directions of guests into cyclodextrins cavities were chosen to select the most favored one (Fig. 2).

The following initial steric conditions were applied for introduction of guest into the CD cavity. The glycosidic oxygen atoms of the cyclodextrin molecule were placed onto the XY plane and their center was defined as the center of the coordination system. The secondary hydroxyl groups of the CD were placed pointing toward the positive Z-axis. For simplicity, the orientation in which NH_2 group of guest points toward primary hydroxyl of CD was called the ''A model'', the other, in which the NH_2 group of the guest points toward the secondary hydroxyl of CD was called the ''B model'', see Fig. 2.

All geometry optimizations of P-methylaminobenzoate derivatives guests and their inclusion complexes by DFT method were performed using B3LYP-D3 through the cc-pVDZ basis set (Figs. 3 and 4). The absence of imaginary frequencies was tested by frequency analyses at the same level of theory to confirm that all optimized structures are true minima.

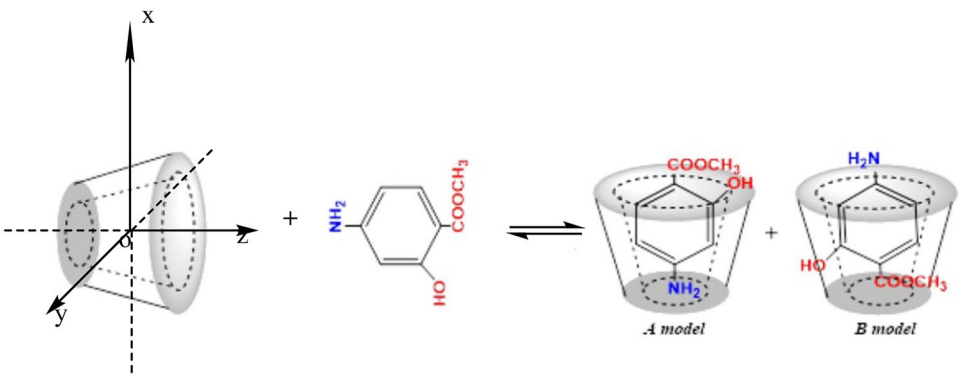

Fig. 2 Possible directions of guest introduction into α and γ-CD

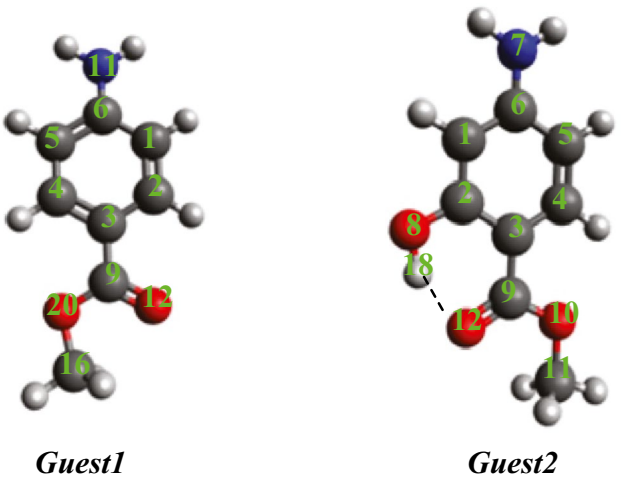

Fig. 3 Ground state optimized structures of methyl 4-aminobenzoate and methyl 4- amino-2-hydroxybenzoate by B3LYP-D3/cc-pVDZ calculations

Absorption and emission spectra were obtained by single point energy and optimization of different species respectively in water by TD-DFT/B3LYP/6-31G(d) with the application of the polarizable continuum model (PCM) with the integral equation formalism variant (IEFPCM).

Intermolecular interactions established between P-methylaminobenzoate derivatives guests and both α and γ-CDs were done by: NBO analysis to quantify intermolecular donor–acceptor interactions, AIM analysis to evaluate the strength of H-bonds interactions and NCI analysis to illustrate repulsion, Van der waals and H-bonds iso-surface interactions.

All calculations were obtained by using Gaussian09 [13], VMD [14] and Multiwfn [15] programs.

Results and Discussion

Energies

In this study, the binding energy between guest and CD is defined in Eq (1) :

$$\Delta E_{binding} = E_{inclusion\ complex} - (E_{host} + E_{guest}) \quad (1)$$

The deformation energy of the guest or the host molecules can be obtained by Eqs. (2) and (3):

$$E_{deformation}(Guest) = E[Guest]_{sp}^{opt} - E[Guest]_{opt} \quad (2)$$

$$E_{deformation}(Host) = E[Host]_{sp}^{opt} - E[Host]_{opt} \quad (3)$$

where $E_{deformation}$ (Guest) stands for the deformation energy of the guest, $E[Guest]_{sp}^{opt}$ is the single point energy of the Guest using its geometry in the optimized complex, and $E[Guest]_{opt}$ is the energy of the optimized geometry of the Guest.

$E_{deformation}$ (Host) stands for the deformation energy of the Host, $E[Host]_{sp}^{opt}$ is the single point energy of the Host using its geometry in the optimized complex, and $E[Guest]_{opt}$ is the energy of the optimized geometry of the Guest.

The calculated binding energies in vacuum and in water for the studied complexes Guest1@α-CD, Guest2@α-CD, Guest1@γ-CD and Guest2@γ-CD computed by B3LYP-D3/cc-pVDZ are summarized and compared in Table 1. As can be seen from Table 1, the negative values of binding energies indicate clearly that the formed complexes are stables and energetically favorable with more negative values in vacuum. For all studied inclusion complexes binding energy of A model is more negative than that of B one in both vacuum and water.

By comparing the results obtained from $\Delta E_{binding}$ in both vacuum and water, we can conclude that Guest1@α-CD is the most favoured inclusion complex with more negative $\Delta E_{binding}$ than the other studied inclusion complexes. This is in contradiction with experimental absorption measurement in solvent mixture of THF-water which found that no inclusion of guest 1 into α-CD. Thus can be explained that theoretical calculations were done only in vacuum and in water and taking in account only the neutral form of Guest1.

According to the calculated binding energies, the formed inclusion complexes are less stables in water than in vacuum.

Deformation energy is also important parameters explaining the internal behavior of both host and guest during inclusion complex process. Generally, from obtained Host and guest deformation summarized in Table 1, Guest1 is more deformed than α and γ-CDs in both vacuum and water. Exceptionally, on the case of Guest1@γ-CD for B model where γ-CD is more deformed. These are explained in next section why emission properties are largely changed after inclusion complex formation.

Contrary to Guest1, the deformation of Guest2 is less than that of α and γ-CDs, only for the inclusion complex Guest2@α-CD for B model. Thus, the substitution by O–H group for Guest2 plays an important role to increase interactions with CDs.

Highest occupied molecular orbital (HOMO) and lowest unoccupied molecular orbital (LUMO) are very important parameters for quantum chemistry. The frontier orbital gap helps to characterize the chemical reactivity and kinetic stability of the molecule. A molecule with a small frontier orbital gap is more polarizable and is generally associated with a high chemical reactivity, low kinetic stability and is also termed as soft molecule. The eigenvalues of HOMO and LUMO and their energy gap reflect the chemical activity of the molecule. A greater HOMO–LUMO energy gap has been taken as an indication of a high stability of the title molecule. As can be clearly seen, HOMO–LUMO energy gap value is in good agreement with binding energies giving that A model is the most stable conformation.

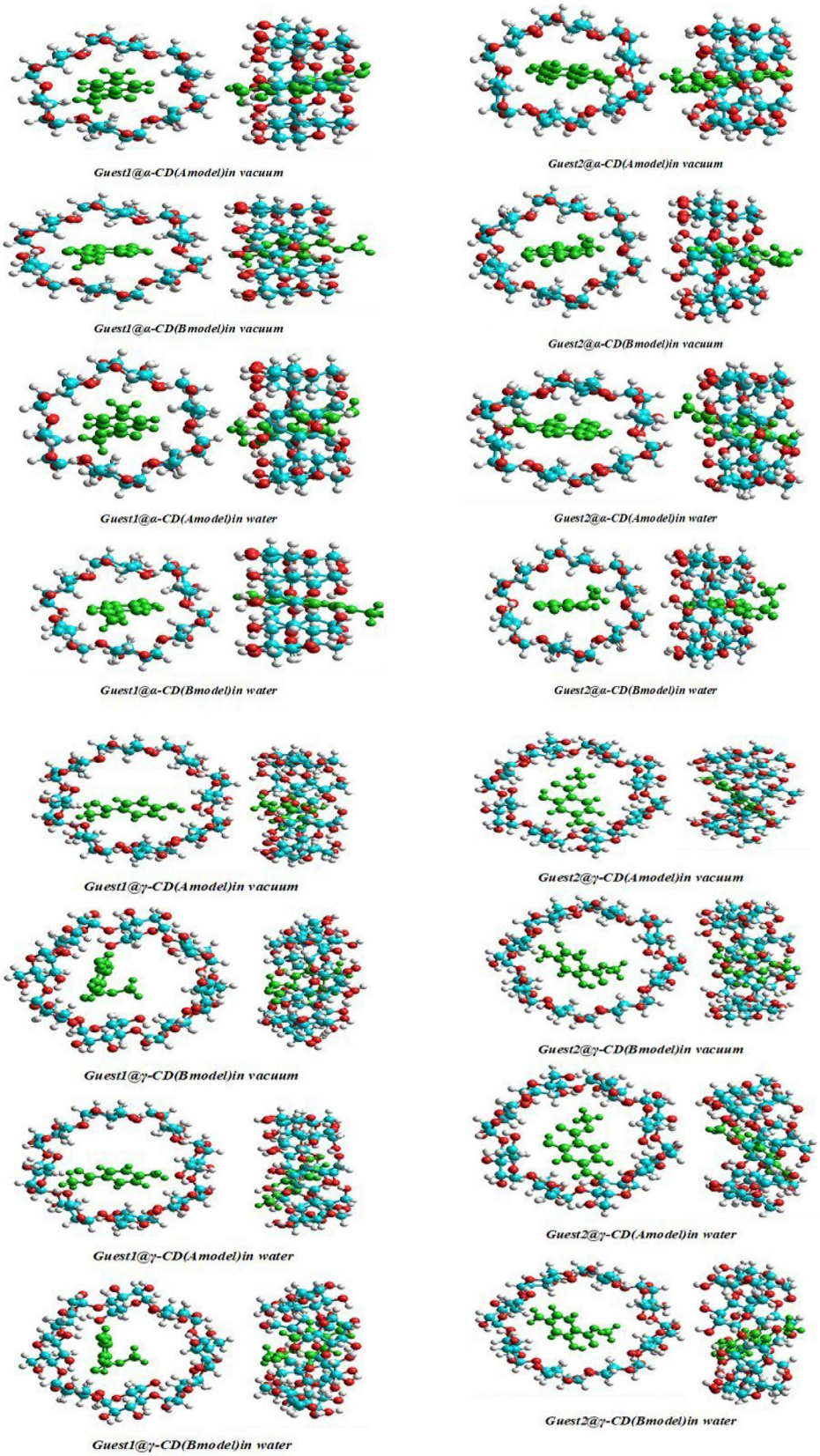

Fig. 4 Ground state optimized structures of methyl 4-aminobenzoate methyl 4-aminobenzoate and methyl 4-amino-2-hydroxybenzoate and their inclusion complexes into α and γ-CD in both vacuum and water obtained from B3LYP-D3/cc-pVDZ calculations

Table 1 Binding energy, Deformation energy, HOMO, LUMO and $\Delta E_{HOMO\text{-}LUMO}$ obtained by B3LYP-D3/cc-pVDZ (d)

	Guest1@α-CD		Guest1@γ-CD		Guest2@α-CD		Guest2@γ-CD	
	A model	B model	A model	B model	A model	B model	A model	B model
In vacuum								
$\Delta E_{binding}$(Kcal /mol)	-57.95	-48.92	-46.30	-39.14	-44.07	-24.36	-38.66	-36.10
$E_{DEF/Host}$ (Kcal /mol)	5.78	3.87	2.85	11.06	8.46	4.78	4.84	3.90
$E_{DEF/Guest}$ (Kcal /mol)	-13.58	-14.52	-14.03	-1.29	2.52	13.40	0.99	1.74
E_{HOMO} (eV)	-5.36	-5.93	-5.57	-6.41	-5.52	-5.75	-5.29	-5.56
E_{LUMO} (eV)	-0.76	-0.89	-0.82	-1.01	-1.01	-0.77	-0.67	-0.73
$\Delta E_{HOMO\text{-}LUMO}$ (eV)	-4.60	-5.04	-4.75	-5.40	-4.51	-4.98	-4.62	-4.82
In water								
$\Delta E_{binding}$(Kcal /mol)	-45.58	-38.62	-36.55	-30.65	-36.91	-21.08	-33.12	-31.53
$E_{DEF/Host}$ (Kcal /mol)	2.95	3.67	2.62	8.78	7.82	5.67	4.55	3.35
$E_{DEF/Guest}$ (Kcal /mol)	-7.92	-9.22	-8.65	2.41	2.58	10.67	0.52	1.68
E_{HOMO} (eV)	-5.79	-5.91	-5.82	-6.34	-5.74	-5.93	-5.67	-5.83
E_{LUMO} (eV)	-1.09	-1.14	-1.12	-1.04	-1.21	-1.23	-1.05	-1.12
$\Delta E_{HOMO\text{-}LUMO}$ (eV)	-4.69	-4.78	-4.70	-5.30	-4.53	-4.70	-4.62	-4.72

Optimized structures on ground state

From Fig. 4, which illustrate geometries of studied inclusion complexes after energy minimization by B3LYP-D3/cc-pVDZ level of computation in vacuum and water for both models A and B. It is clearly observed in all geometries that P-methylaminobenzoate derivatives (Guest1 and Guest2) are deeply included in α and γ-CD cavities. It is remarkable that in α-CD, both aromatic rings plan of methyl 4-aminobenzoate and methyl 4- amino-2-hydroxybenzoate are perpendicular to xy plan of α-CD in vacuum and in water. However, in γ-CD, the two guests are positioned differently than that on α-CD that is due to the large volume of γ –CD cavity. This allows the guest molecule to rotate freely and seek the right position inside the cavity to establish a large number of stabilizing intermolecular interactions. To identify the nature of this intermolecular interactions NBO, NCI and AIM were successfully performed.

The NBO analysis, which quantifies the stabilizing energy $E^{(2)}$ between the two components of the studied inclusion complexes, clearly showed the transfer of charge (donor–acceptor) between the bonding and anti-bonding orbitals. The interactions (donor–acceptor) observed are of type BD → BD*, BD → RY* and LP → BD* (Table S1).

AIM analysis was also applied to study existence of bond critical point (BCP) between the P-methylaminobenzoate derivatives (Guest1 and Guest2) and α and γ-CD. In all studied inclusion complexes, the ρ(r) and $\nabla^2\rho(r)$ values are positive (Table S2) and in agreement with the principles for H-bond formation proposed by Koch and Popelier [16].

3D isosurface obtained by NCI analysis support NBO and AIM analysis by showing the presence of blue and green colors at the surface contact between studied dyes and CDs (Fig. S1) and approving the establishment of intermolecular van der Waals and H-bonds interactions respectively.

Analysis of absorption and emission spectra

For our study, we have chosen A model the most stable inclusion complex in water to perform TD-DFT calculations. TD-DFT/B3LYP/6-31G(d) calculations have been successfully employed to give more insight about UV–visible spectra properties [17–19]. Figure 5 illustrates absorptions bands of methyl 4-aminobenzoate, methyl 4- amino-2-hydroxybenzoate and their inclusion complexes into α and γ-CD water (IEFPCM model).

Analysis of the simulated absorption spectra of the two derivatives of P-methylaminobenzoate Guest1 and Guest2 and their inclusion complexes in α and γ-CDs revealed that i) for Guest1, the presence of a band broad absorption range located in the 180–280 nm range. The maximum of this absorption λ_{abs} is 228 nm which corresponds to the H → L + 2 transition with a contribution of 80% and oscillator strength f = 0.329.

According to the literature [11], the experimental electronic absorption spectrum of Guest1 in water exhibited two absorption bands: strong long-wavelength band in region of 260-340 nm and weaker short-wavelength in 220-250 nm. The difference between experimental and calculated absorption spectra can be explained by intramolecular interaction between functional groups NH_2 and $COOCH_3$ of G1 and water solvent (dipole–dipole and hydrogen-bonds) in the ground state.

ii) But when interacting with α and γ-CDs, λ_{abs} is shifted to longer wavelengths; the absorption spectrum of Guest1@α-CD (Fig. 5) shows two absorption bands confirming the formation of the Guest1@α-CD inclusion complex. The first absorption band has a lower intensity than the second band, the two absorption maxima are different from that of free methyl 4-aminobenzoate which

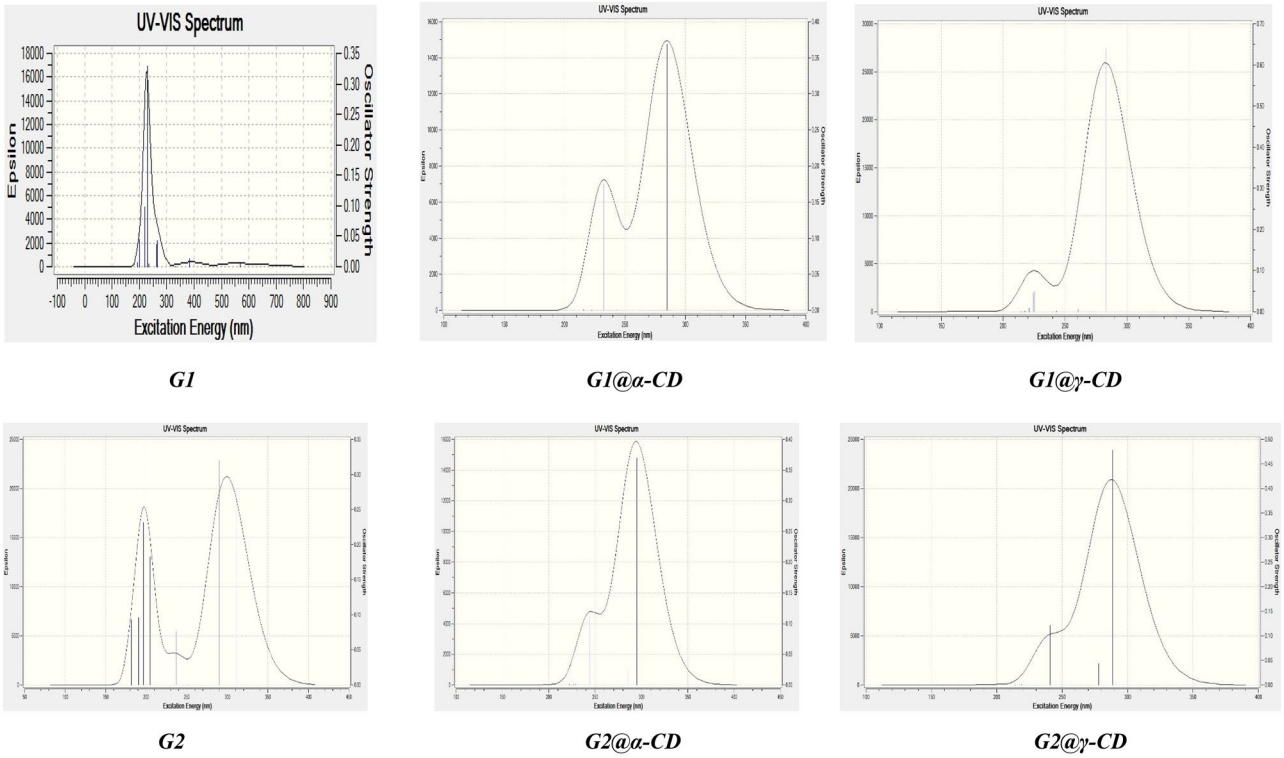

Fig. 5 Simulated electronic absorption spectra of P-methylaminobenzoate derivatives and their inclusions complexes using the TD-DFT-B3LYP/6-31G (d) method

are observed at (232 nm, f = 0.1760 and H → L + 3) and (284 nm, f = 0.3687and H → L) respectively. The simulated absorption spectra of Guest1@α-CD inclusion complex is largely different from practical one which illustrate no clear isobestic point in the normalized absorption spectra which rule out the formation of well 1:1 Guest1@α-CD inclusion complex. This large difference between simulated and experimental can be explained by the level of theory used to estimate absorption spectra.

iii) The spectrum of Guest1@γ-CD has two absorption bands; the smallest one has to low intensity compared to that of the inclusion complex Guest1@α -CD. λabs = 224 nm (f = 0.0463 and H → L + 4) corresponds to the absorption maximum of the small band while λabs = 282 nm (f = 0.6387 and H → L) corresponds to the intense band. The calculated absorption spectra of Guest1@γ-CD inclusion complex present two absorption different centers, which agree well with experimental results.

vi) In the case of methyl 4- amino-2-hydroxybenzoate (Guest2), two broad absorption bands are observed with intense oscillator strength (f) suggesting the establishment of intramolecular hydrogen bond, the first which corresponds to a vertical transition is located at λabs = 196 nm (f = 0.2317 and H → L + 5) while the second band is at λ_{abs} = 289 nm (f = 0.3194 and H → L + 1). Experimentally, these two bands were observed in regions 220-250 nm and 260-340 nm for weaker short and strong long bands respectively.

v) A bathochromic effect is observed during the formation of the Guest2@α-CD and Guest2@γ-CD inclusion complexes. λabs of the intense band is observed at λabs = 294 nm (f = 0.3693 and H → L) and λabs = 288 nm (f = 0.4779 and H → L) for Guest2@α-CD and Guest2@γ-CD respectively.

By comparing the intensities of the two inclusion complexes, we find that the absorption band of the Guest2@γ-CD complex is more intense than that of the Guest2@α-CD complex, which is experimentally proven [11].

Figure 6 presents calculated fluorescence spectra of methyl 4-aminobenzoate and methyl 4- amino-2-hydroxybenzoate in water. The emission spectrum of **Guest 1** possesses only fluorescence band (λem = 321.92 nm locally excited), the presence of one emission band of methyl 4-aminobenzoate and methyl 4- amino-2-hydroxybenzoate is confirmed experimentally in mixture solvent THF-water at $X_{water} < 0.4$.

Simulated fluorescence spectra of **Guest 2** contains two partially overlapping bands i.e., short-wavelength (λem = 384 nm, locally excited) fluorescence, and intramolecular proton transfer band (λem = 570 nm, ESIPT).From experimental results, the ESIPT fluorescence is full-width at half maximum value increases by about 25% when the Xwater is increased from 0 to 1.

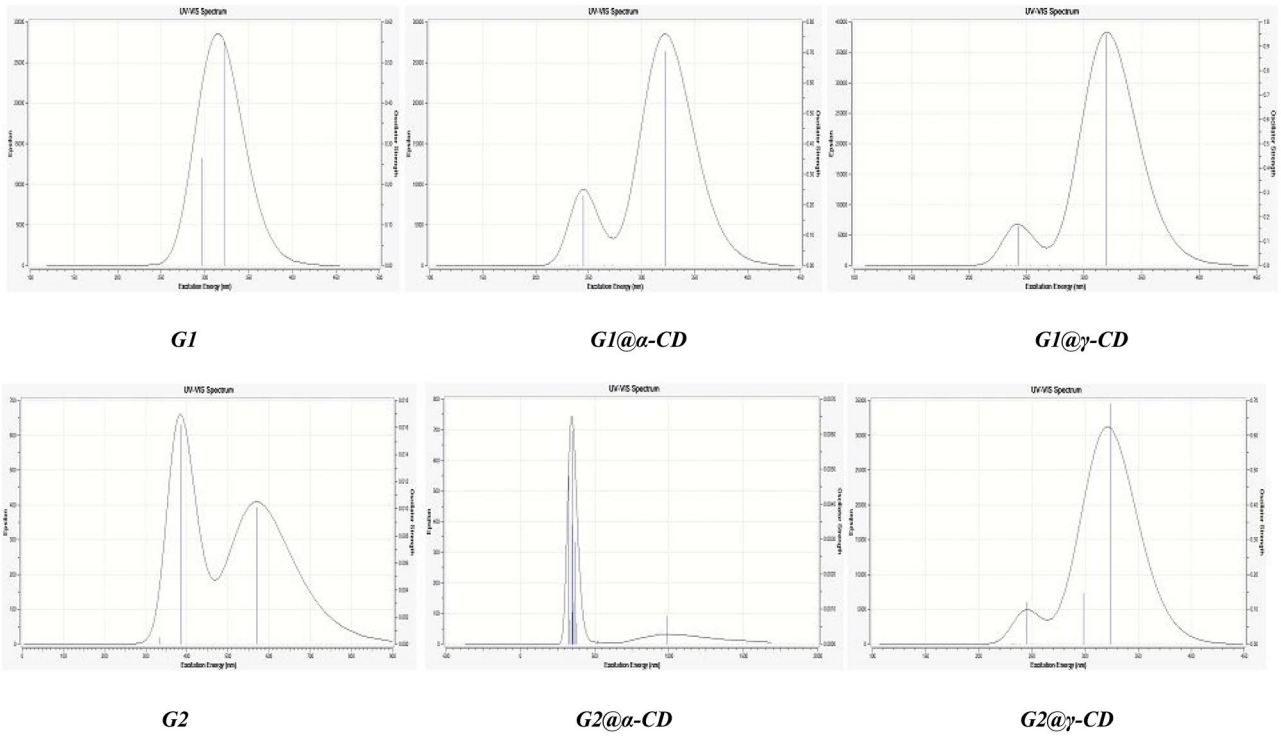

Fig. 6 Simulated emission spectra of P-methylaminobenzoate derivatives and their inclusions complexes using the TD-DFT/B3LYP/6-31G (d) method

The analysis of the fluorescence emission of inclusion complexes Guest1@α-CD, Guest1@γ-CD, Guest2@α-CD and Guest2@γ-CD showed the presence of two emission bands corresponding to the presence of two emitters centers: the free fluorophore and its inclusion complex with α or γ-CD.

The first band which is the least intense is observed at wavelengths of 245, 242 and 245 nm for Guest1@α-CD, Guest1@γ-CD and Guest2@γ-CD respectively with low oscillator strength. While the Guest2@α-CD inclusion complex presents a single low intensity band which is found at λem = 346 nm with f = 0.0034. The important emission behavior change observed between free Guest2 and its inclusion complex with α-CD is due to its conformational changes in excited states after inclusion complex formation especially loss of intramolecular H-bond established between O12···H18 (1.578Å in GS and 2.956 Å in ES) and establishment of great number of interactions between methyl 4- amino-2-hydroxybenzoate and α-CD.

The most intense band is located at wavelengths of (λem = 322 nm, f = 0.7045) (λem = 319 nm, f = 0.9466) and (λem = 324 nm, f = 0.6909) for Guest1@α-CD, Guest1@γ-CD and Guest2@γ-CD respectively with strong oscillator strength. The comparison between calculated and experimental emission spectra of the studied inclusion complexes shows large similarity only for Guest2@α-CD, the formation of inclusion complexes between Guest1 and Guest2 was confirmed in excited states. we can say that

Table 2 Absorption, emission and Stocks shifts of studied dyes and their inclusion complexes (nm)

	λ_{abs}	λ_{em}	$\Delta(\lambda_{abs}- \lambda_{em})$
Guest1	228.53	321.92	93.39
Guest1@α-CD	284.85	322.26	37.41
Guest1@γ-CD	282.85	319.77	36.92
Guest 2	289.86	384.69	94.83
Guest2@α-CD	294.93	346.36	51.43
Guest2@γ-CD	288.51	324.4	35.89

Table 3 Dipole moment (μ, Debye) of studied dyes and their inclusion complexes

	Ground state	Excited state
Guest1	8.468	8.478
Guest1@α-CD	8.355	9.098
Guest1@γ-CD	13.670	15.123
Guest 2	5.671	5.678
Guest2@α-CD	6.231	10.558
Guest2@γ-CD	14.519	17.449

Table 4 Comparison between geometrical parameters of ground and excited states of methyl 4-aminobenzoate and methyl 4- amino-2-hydroxybenzoate (B3LYP/6-31G(d)

	Guest1		Guest1@α-CD		Guest1@γ-CD			Guest2		Guest2@α-CD		Guest2@γ-CD	
	GS	ES	GS	ES	GS	ES		GS	ES	GS	ES	GS	ES
(Å)							(Å)						
C1-C2	1.392	1.391	1.385	1.387	1.399	1.382	**C1-C2**	1.397	1.382	1.388	1.377	1.395	1.386
C2-C3	1.407	1.408	1.405	1.432	1.407	1.435	**C2-C3**	1.426	1.472	1.422	1.426	1.426	1.448
C3-C4	1.401	1.402	1.405	1.432	1.408	1.434	**C3-C4**	1.411	1.400	1.413	1.407	1.415	1.425
C4-C5	1.396	1.396	1.387	1.388	1.386	1.389	**C4-C5**	1.380	1.422	1.377	1.382	1.378	1.402
C5-C6	1.414	1.396	1.413	1.428	1.414	1.411	**C5-C6**	1.421	1.426	1.422	1.438	1.425	1.411
C1-C6	1.414	1.417	1.411	1.425	1.414	1.413	**C1-C6**	1.404	1.417	1.410	1.425	1.409	1.425
C6-N11	1.377	1.375	1.377	1.379	1.377	1.402	**C6-N7**	1.368	1.377	1.359	1.347	1.362	1.402
C3-C9	1.515	1.514	1.469	1.458	1.474	1.413	**C3-C9**	1.457	1.455	1.449	1.505	1.453	1.433
C9-O12	1.364	1.362	1.221	1.280	1.220	1.306	**C2-O8**	1.341	1.362	1.355	1.376	1.349	1.387
C9-O20	1.425	1.426	1.367	1.413	1.360	1.443	**C9-O12**	1.236	1.305	1.241	1.317	1.240	1.330
O20-C16	1.464	1.464	1.434	1.461	1.436	1.451	**C9-O10**	1.349	1.387	1.351	1.442	1.351	1.410
(°)							**O10-C11**	1.435	1.463	1.438	1.460	1.433	1.460
C3-C9-O12	116.323	116.029	126.015	125.873	124.932	128.524	**O12···H18**	1.687	1.578	1.578	2.956	1.724	1.573
C3-C9-O20	114.980	114.949	112.323	112.564	112.775	113.566	(°)						
O12-C9-O20	109.602	109.897	121.651	121.861	122.269	117.908	**C3-C9-O12**	124.327	124.133	124.701	118.165	124.851	124.759
C9-O20-C16	114.212	114.271	116.185	116.885	115.537	115.920	**C9-O10-C11**	115.678	116.941	117.429	114.835	116.078	117.413
							O12-C9-O10	121.233	121.302	121.299	119.876	121.297	120.526
							C3-C9-O10	114.439	114.563	113.999	107.174	113.850	114.713

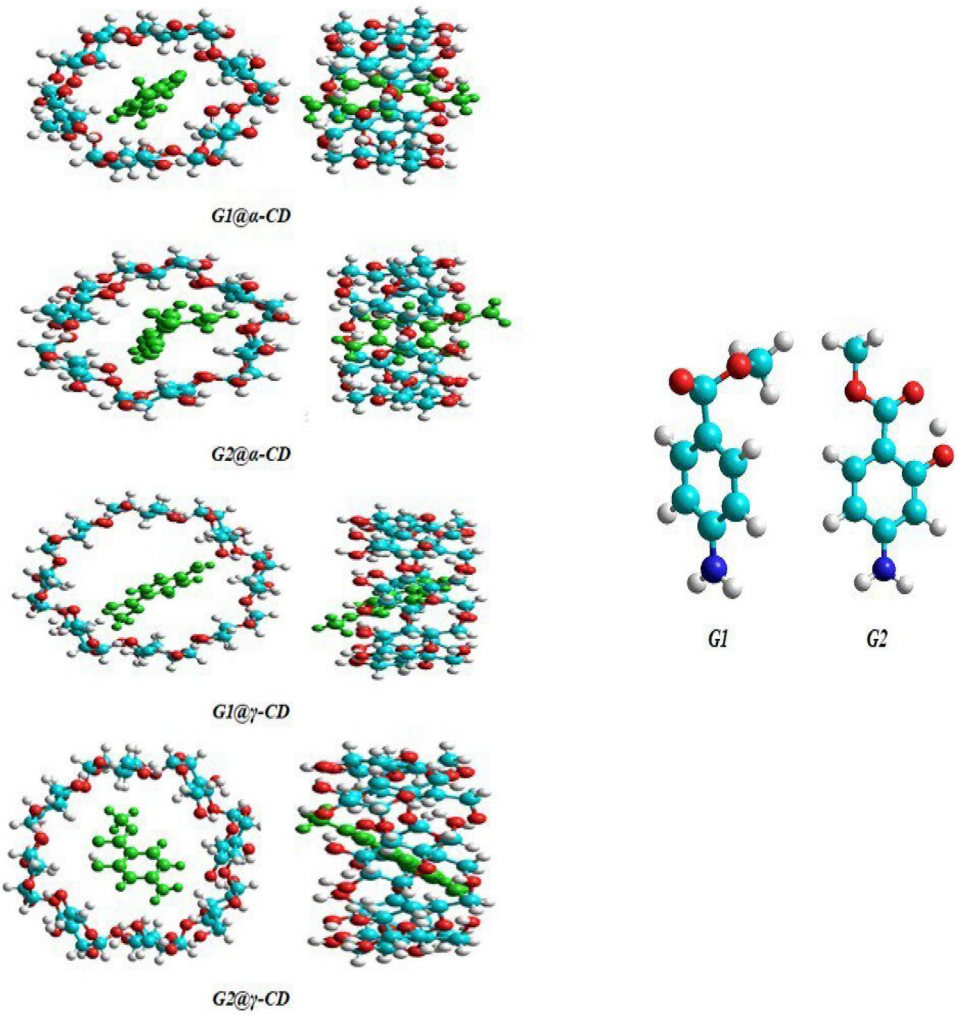

Fig. 7 Excited state optimized structures of methyl 4-aminobenzoate and methyl 4-amino-2-hydroxybenzoate and their inclusion complexes into α and γ-CD in water obtained by B3LYP/6-31G (d) calculations

the fluorescence spectroscopy is a good tool for characterizing molecular environments, which is touchier than the vast majority of other spectroscopic techniques. It is used because of her particularity, high selectivity and low recognition limits.

From Table 2, the Stokes Shift of studied dyes and their inclusions complexes is calculated by taking the wavelength difference between the λabs of the absorption and the λem of the emission peak. The relatively high values of stokes shift are obtained for Guest2 (94.83 nm) and the

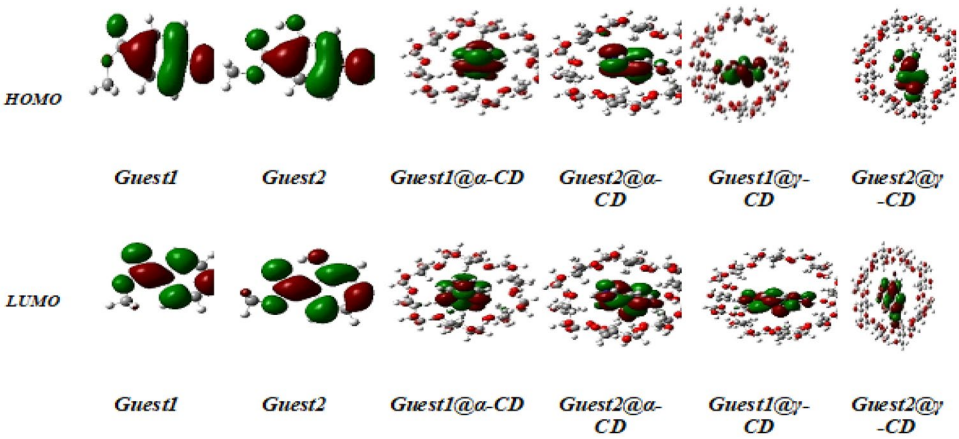

Fig. 8 Illustration of frontier molecular orbitals HOMO and LUMO of studied species

lows value are obtained for Guest2@γ-CD (35.89 nm). In the presence of α and γ-CD, the values of Stokes Shift are decreased as a result; we can conclude that photo excitation causes conformational changes between ground and excited states of dyes inclusion complexes. The following order is established: $\Delta(\lambda_{abs}- \lambda_{em})$ Guest2@γ-CD < $\Delta(\lambda_{abs}- \lambda_{em})$ Guest1@γ-CD < $\Delta(\lambda_{abs}- \lambda_{em})$Guest1@α-CD < $\Delta(\lambda_{abs}- \lambda_{em})$ Guest2@α-CD < $\Delta(\lambda_{abs}- \lambda_{em})$Guest1 < $\Delta(\lambda_{abs}- \lambda_{em})$ Guest 2.

We can also note that relatively high values of Stocks Shift (SS) are obtained on free Guest1 (93.39) and Guest2 (94.83), this indicate that the compounds which have a weak Stocks Shift present a minimal conformational reorganization between ground state and excited state.

The dipole moment is an important parameter reflecting distribution of electronic charges in the molecules and affecting molecular geometries. From Table 3 in excited state, the dipole moment is larger than that in ground state giving that the dyes compounds are more polarized in the excited state. The highest values are found with guest1@γ-CD and guest2@γ-CD by 15.123 and 17.449 respectively.

The significantly difference of the magnitude of induced dipole moment between ground and excited states is due to the formation of intermolecular interactions between dyes and both α and γ-CDs especially hydrogen bonds in excited state.

In Table 4, there is comparison of angles and bond lengths between ground state (S0) and the first excited state (S1) of free and inclusion form of P-methylaminobenzoate derivatives into α and γ-cyclodextrins calculated by B3LYP/6-31G(d) methods. The most significant difference between S1 and S0 geometry is observed with guest2 into α-CD, the valence angles of Guest 2 in ground state C3-C9-O12(124.701), C9-O10-C11(117.429), O12-C9-O10(121.299) and C3-C9-O10(113.999) are changed to 118.165, 114.835, 119.876 and 107.174 respectively in excited state. There are also remarkable difference of interatomic distance between O12···H18 which is of 1.578Å in S0 and 2.956 Å in S1 for Guest2@α-CD.

As it can be seen in Table 4, the bond lengths differences do not exceed 0.091Å. For free Guest1, C5-C6 bond length is 0.018 Å in S0 larger than that in S1, while C9-O12 is smaller in S0 than in S1 by 0.059 and 0.086 for Guest1@α-CD and Guest1@γ-CD respectively. Thus, C9-O12 bond length in the formed inclusion complex between Guest1 and both α and γ-CD is more affected in ground and excited state do to intermolecular interactions.

Generally, in comparison to the ground state, the geometry of both studied fluorophore in the lowest singlet excited state undergoes deformation especially after inclusion complex formation with α and γ-cyclodextrins (Fig. 7).

Frontier Molecular orbitals

In order to shed more light on the effect of inclusion complexation on the molecular properties of both dyes, it is necessary to investigate the nature of molecular orbitals (MOs) of methyl 4-aminobenzoate and methyl 4- amino-2-hydroxybenzoate before and after complexation with α and γ-CDs.

From Fig. 8, it is clearly showed that HOMO of P-methylaminobenzoate derivatives is the π molecular orbital of C–C, lone pair of N and oxygen atoms. For LUMO molecular orbital, the π* of aromatic rings is the first excited states during absorption process. Analysis of molecular orbitals (MOs) that give the major contribution to these transitions have shown that most of them are π-π* transitions.

For dyes inclusions complexes both HOMO and LUMO orbital's are located on P-methylaminobenzoate derivatives giving that the majors vertical transitions are intramolecular excitations.

Conclusion

The application of the DFT and TD-DFT methods with the bases cc-pVDZ and 6-31G(d) respectively in water (IEFPCEM model) on the two fluorophores methyl 4-aminobenzoate methyl 4-aminobenzoate (Guest 1) and methyl 4- amino-2-hydroxybenzoate (Guest2) and their inclusions complexes with α and γ-cyclodextrins for studying their excited and ground state geometries as well as their absorption and emission spectra has shown that:

- The two studied fluorophores forms with α and γ-CDs 1:1 stables inclusion complexes.
- For the absorption spectra, the Guest1 has a single absorption band; the spectrum of Guest 2 is formed of two separate bands while their inclusion complexes are similar and consist of the overlap of two absorption bands, which confirm the formation of inclusion complexes.
- Fluorescence properties are different between free and included forms of the two fluorophores, for Guest1 there is one emission band, the Guest2 exhibit two emission bands (LE and ESIPT) while in the inclusion complexes two overlapping bands were observed suggesting the presence of two emitter's centers.
- The modification of geometrical parameters in excited states clearly indicate the conformational changes of the studied dyes in excited state especially in the included form because stronger intermolecular interactions were established.

Supplementary Information The online version contains supplementary material available at https://doi.org/10.1007/s10895-023-03146-x.

Acknowledgements The investigation was supported by the Algerian Ministry of Higher Education and Scientific Research (project PRFU B00L01UN240120200002).

Authors' Contributions Badi Sonia performed the calculation and analyse the results. Madi fatiha wrote the manuscript. Nouar Leila revise the manuscript. Gheid abdelhak supervised the work.

Funding Not applicable.

Data Availability Not applicable.

Declarations

Ethical Approval Not applicable.

Consent for Publication All authors mentioned in the manuscript have given consent for submission and subsequent publication of the manuscript.

Conflict of Interests The authors have declared no conflict of interest.

References

1. Holkar A, Ghodke S, Bangde P et al (2022) Fluorescence-Based Detection of Cholesterol Using Inclusion Complex of Hydroxypropyl-β-Cyclodextrin and L-Tryptophan as the Fluorescence Probe. J Pharm Innov 17:170–179. https://doi.org/10.1007/s12247-020-09503-8
2. Ay U, Sarlı SE (2018) Investigation by Fluorescence Technique of the Quenching Effect of Co^{2+} and Mn^{2+} Transition Metals, on Naphthalene-Methyl-Beta-Cyclodextrin Host-Guest Inclusion Complex. J Fluoresc 28:1371–1378. https://doi.org/10.1007/s10895-018-2301-9
3. Miskolczy Z, Harangozó JG, Biczók L et al (2014) Effect of torsional isomerization and inclusion complex formation with cucurbit[7]uril on the fluorescence of 6-methoxy-1-methylquinolinium. Photochem Photobiol Sci 13:499–508. https://doi.org/10.1039/c3pp50307k
4. Mendy A, Thiaré DD, Bodian EHT et al (2019) Inclusion Complex of *O*-phthalaldehyde-Buprofezin with Dimethyl-β-Cyclodextrin Using Thermochemically-Induced Fluorescence Derivatization (TIFD) Method and its Analytical Application in Waters. J Fluoresc 29:515–522. https://doi.org/10.1007/s10895-019-02386-0
5. Mendy A, Thiaré DD, Sarr I et al (2019) Inclusion Complex of *o*-Phthalaldehyde-Metolachlor with Cyclodextrins Using the Thermochemically-Induced Fluorescence Derivatization (TIFD) Method and Its Analytical Application in Waters. J Solution Chem 48:502–514. https://doi.org/10.1007/s10953-019-00862-6
6. Sueishi Y, Matsumoto Y, Sohama J et al (2019) Distinctive effects on fluorescence quantum yields of 4-substituted *N*-methylphthalimides by inclusion complexation with β-cyclodextrins. J Incl Phenom Macrocycl Chem 93:275–281. https://doi.org/10.1007/s10847-018-00877-4
7. Sueishi Y, Hagiwara S, Inazumi N et al (2021) Inclusion complexation of 4′,6-diamidino-2-phenylindole (DAPI) with cucurbit[7]uril and cyclodextrins (native β-, 2,6-*di*-*O*-methylated β-, and γ-cyclodextrin): characteristic inclusion behaviour and fluorescence enhancement. J Incl Phenom Macrocycl Chem 99:209–216. https://doi.org/10.1007/s10847-020-01042-6
8. Zidane S, Maiza A, Bouleghlem H et al (2019) Inclusion complex of Tramadol in β-cyclodextrin enhances fluorescence by preventing self-quenching. J Incl Phenom Macrocycl Chem 93:253–264. https://doi.org/10.1007/s10847-018-0874-1
9. Maged A. El-K, Hani S. El-Gazawy HS (2003) Spectral study and global analysis of fluorescence decays of the inclusion complexes of 2-amino-4,6-dimethyl pyrimidine with α- and γ-cyclodextrins. J Photochem Photobiol 155:151–156
10. Marek J (2012) Effect of α- and β-cyclodextrins on the intramolecular charge transfer and intramolecular proton transfer fluorescence of methyl o-hydroxy p-dimethylaminobenzoate. Spectrochimica Acta Part A 93:169–175. https://doi.org/10.1016/j.saa.2012.02.112
11. Karolina B, Marek J (2018) Spectroscopic studies of inclusion complexation between ortho derivatives of *p*-methylaminobenzoate and α- and γ-cyclodextrins. J Mol Liq 265:140–150. https://doi.org/10.1016/j.molliq.2018.05.120
12. Djellala et al (2020) Investigation of intermolecular interactions in inclusion complexes of pyroquilon with cucurbit[*n*]urils ($n = 7,8$) using DFT-D3 correction dispersion. J Mol Liq 309:L113233. https://doi.org/10.1016/j.molliq.2020.113233
13. Frisch MJ, Trucks GW, Schlegel HB, Scuseria GE, Robb MA, Cheeseman JR, Scalmani G, Barone V, Mennucci B, Petersson GA, Nakatsuji H, Caricato M, Li X, Hratchian HP, Izmaylov AF, Bloino J, Zheng G, Sonnenberg JL, Hada M, Ehara M, Toyota K, Fukuda R, Hasegawa J, Ishida M, Nakajima T, Honda Y, Kitao O, Nakai H, Vreven T, Montgomery, JA Jr Peralta JE, Ogliaro F, Bearpark MJ, Heyd J, Brothers EN, Kudin KN, Staroverov VN, Kobayashi R, Normand J, Raghavachari K, Rendell AP, Burant JC, Iyengar SS, Cossi JM, Rega N, Millam NJ, Klene M, Knox JE, Cross JB, Bakken V, Adamo C, Jaramillo J, Gomperts R, Stratmann RE, Yazyev O, Austin AJ, Cammi R, Pomelli C, Ochterski JW, Martin RL, Morokuma K, Zakrzewski VG, Voth GA, Salvador P, Dannenberg JJ, Dapprich S, Daniels DA, Farkas D, Foresman JB, Ortiz JV, Cioslowski J, Fox DJ (2013) Tomasi Title Suppressed Due to Excessive Length 15 Gaussian 09, revision A.01
14. Humphrey W, Dalke A, Schulten K (1996) VMD: visual molecular dynamics. J Mol Graph 14(1):33–38. https://doi.org/10.1016/0263-7855(96)00018-5
15. Lu T, Chen F (2011) Multiwfn: A multifunctional wavefunction analyzer. J Comput Chem 33:580. https://doi.org/10.1002/jcc.22885
16. Koch U, Popelier PLA (1995) Characterization of C-H-O hydrogen bonds on the basis of the charge density. J Phys Chem 99(24):9747–9754
17. Stratmann RE, Scuseria GE, Frisch MJ (1998) An efcient implementation of time-dependent density-functional theory for the calculation of excitation energies of large molecules. J Chem Phys 109(19):8218–8224. https://doi.org/10.1063/1.477483
18. Fan Gh, Han Kl, He Gz (2013) Time-dependent density functional-based tight-bind method efficiently implemented with OpenMP parallel and GPU acceleration. Chin J Chem Phys 26(6):635–645. https://doi.org/10.1063/1674-0068/26/06/635-645
19. Ma Y, Feng L, Liu J et al (2020) DFT/TDDFT investigation on the D–π–A type molecule probes 4-(5-R-thiophen-2-yl)-2-isobutyl-2H-[1,2,3]triazolo[4,5-e][1,2,4] triazolo[1,5-a]pyrimidines: fluorescence sensing mechanism and roles of weak interactions. Theor Chem Acc 139:11. https://doi.org/10.1007/s00214-019-2520-4